

This is the accepted manuscript made available via CHORUS. The article has been published as:

Current and future constraints on dark matter from prompt and inverse-Compton photon emission in the isotropic diffuse gamma-ray background

Kevork N. Abazajian, Steve Blanchet, and J. Patrick Harding

Phys. Rev. D **85**, 043509 — Published 10 February 2012

DOI: [10.1103/PhysRevD.85.043509](https://doi.org/10.1103/PhysRevD.85.043509)

Current and Future Constraints on Dark Matter from Prompt and Inverse-Compton Photon Emission in the Isotropic Diffuse Gamma ray Background

Kevork N. Abazajian^{1,2,*}, Steve Blanchet^{2,3,†} and J. Patrick Harding^{1,2‡}

¹*Department of Physics and Astronomy, University of California, Irvine, Irvine, California 92697 USA*

²*Maryland Center for Fundamental Physics & Joint Space-Science Institute,*

Department of Physics, University of Maryland, College Park, Maryland 20742 USA and

³*Instituto de Física Teórica, IFT-UAM/CSIC Nicolas Cabrera 15, UAM Cantoblanco, 28049 Madrid, Spain*

We perform a detailed examination of current constraints on annihilating and decaying dark matter models from both prompt and inverse-Compton emission photons, including both model-dependent and model-independent bounds. We also show that the observed isotropic Diffuse Gamma Ray Background (DGRB), which provides one of the most conservative constraints on models of annihilating weak-scale dark matter particles, may enhance its sensitivity by a factor of ~ 2 to 3 (95% CL) as the Fermi-LAT experiment resolves DGRB contributing blazar sources with five years of observation. For our forecasts, we employ the results of constraints to the luminosity-dependent density evolution plus blazar spectral energy distribution sequence model, which is constrained by the DGRB and blazar source count distribution function.

PACS numbers: 95.35.+d, 95.55.Ka

I. INTRODUCTION

The existence of cosmological dark matter is well established by observations of galaxy clusters, galaxy rotation curves, the cosmic microwave background (CMB) and large-scale structure, though its nature remains a fundamental problem in cosmology and particle physics. There exists an abundance of particle candidates which could account for the dark matter (for a review, see, e.g. [1]). For a class of particles with weak-scale interaction and weak-scale particle mass, Weakly Interacting Massive Particles (WIMPs), their production in the early universe in thermal processes naturally produces the observed dark matter density, largely independent of the particle mass.

Thermal freeze-out predicts a canonical annihilation rate of $\langle\sigma_A v\rangle \approx 3 \times 10^{-26} \text{ cm}^3 \text{ s}^{-1}$. This predicted annihilation rate in Standard Model channels leads to energetic gamma ray production in the hadronization of quarks, the Higgs or gauge bosons, through bremsstrahlung in the case of the lighter leptons, or directly to two gammas through higher order processes. The DGRB was forecast to be one of the most robust constraints on annihilating WIMP dark matter [2]. Due to a more conservative model for the extragalactic dark matter signal, the conservative limits on dark matter annihilation presented by the Fermi-LAT collaboration from the one-year observation of the DGRB [3, 4] were weaker than pre-launch estimates [2]. On the other hand, it was shown that the DGRB has an irreducible contribution from the Milky

Way Galactic dark matter halo [5] that is greater in amplitude than the conservative estimates of the extragalactic contribution, and correspondingly has more stringent limits over many annihilation channels [6]. This irreducible, isotropic component is due to the fact that annihilating or decaying dark matter in the Milky Way halo has an isotropic component equal to the minimum of the annihilation or decay signal. This minimum is equal to the amount toward the anti-Galactic Center.

The isotropic DGRB has several potential astrophysical source contributions, including blazars [7–10], starburst galaxies [11] and millisecond pulsars [12]. The only model that successfully predicts the shape and amplitude of the DGRB over all energies is the luminosity dependent density evolution (LDDE) blazar spectral energy density (SED) sequence model with an active galactic nuclei (AGN) contribution [13, 14]. The SED sequence model matches the shape of the observed blazar SED’s luminosity dependence [15]. Ref. [13] reproduces well the DGRB as observed by Fermi-LAT, while several other analyses under-produce the DGRB from blazars. Ref. [13] estimates that $\gtrsim 98\%$ of the blazar flux contributing to the DGRB will be resolved in the 5-year Fermi-LAT survey. Prior work that under-produces the DGRB uses a single power-law for the spectrum of all blazars instead of the observed SED sequence for blazars, e.g. [16]. Other recent work with varied blazar population models, including spectral shape variation [17], possible point source confusion [18], and BL Lac dominance of the unresolved portion [19] also find that a substantial portion of the DGRB could arise from the blazar population.

There may also be an unmodeled, unreduced isotropic Galactic component to the DGRB [3, 4]. It should be noted that two things could happen if there is a presently

* kevork@uci.edu

† steve.blanchet@epfl.ch

‡ hard0923@umd.edu

unremoved Galactic isotropic diffuse component: one, it is detected, modeled, and removed, which will make future constraints stronger; or, two, it remains a systematic diffuse background, which means our starting assumption of an LDDE SED-sequence model is not the correct model for the DGRB. However, this uncertainty cannot be removed without further observational analysis.

Below, we calculate and show the current constraints from the DGRB on dark matter annihilation and decay gamma rays from the prompt as well as inverse-Compton components. In addition, when adopting the LDDE plus SED-sequence model forecasts of the Fermi-LAT resolved DGRB, future observations will extend the reach of Fermi-LAT sensitivity to dark matter typically by a factor of two to three. We explore in detail the forecasts on standard WIMP dark matter and leptonic-channel motivated models [20] including Asymmetric Dark Matter models [21], nonthermal wino-like dark matter [22], and decaying dark matter [23], as well as models of light (~ 8 GeV) WIMP dark matter in scalar dark matter models [24, 25]. The resolution of the DGRB into point source blazars will reduce the DGRB amplitude and ultimately enhance the limits on annihilation in WIMP dark matter models.

In a companion paper, Ref. [14] (ABH2), we constrain our adopted SED sequence model using the observed DGRB spectrum as well as the observed blazar source count distribution function, dN/dF . In agreement with Ref. [13], ABH2 found that $\gtrsim 95\%$ of the flux from blazars will be resolved with 5 years of Fermi-LAT observation. The resolution of the DGRB is in fact similar to the resolution of the cosmic X-ray background observed by *Chandra*, which in turn provided stringent constraints on decaying light sterile neutrino dark matter [26].

The work presented here advances previous work on prompt gamma-ray emission in annihilating dark matter (e.g., [6]) by including the enhanced constraints and sensitivity from inverse-Compton (IC) emission present in the Fermi-LAT observation of the DGRB as well as forecasts of the improvement of this sensitivity. In addition, we go beyond previous analyses of IC emission enhancement of the extragalactic and Galactic signals (e.g., [23, 27]) by applying the IC enhancement in the Fermi-LAT observation of the DGRB and its forecast improvement.

II. THE BLAZAR POPULATION AND SED SEQUENCE MODEL

The SED sequence model specifies the cosmological blazar spatial distribution and spectrum for a given blazar luminosity. It is based on the observed evolution of the peak flux in synchrotron and IC emission with luminosity. The luminosity-dependent density evolution model specifies the gamma ray luminosity function of blazars through a fraction of the total AGN population and its X-ray luminosity function. Our blazar pop-

ulation and SED sequence model in ABH2 successfully reproduces the observed DGRB and blazar source count dN/dF .

Our model is a modification of that by Inoue & Totani [8], and is detailed in ABH2. We provide a summary here. The bolometric blazar jet luminosity P and disk X-ray luminosity L_X are related by $P = 10^9 L_X$. The blazar gamma ray redshift-dependent luminosity function is given as a fraction κ of the AGN X-ray luminosity function (XLF), $\rho_\gamma(L_\gamma, z) = \kappa(dL_X/dL_\gamma)\rho_X(L_X, z)$. We adopt the AGN XLF of Ueda et al. [28]. The main fit parameter in the XLF is the faint-end slope index, γ_1 . The model also includes a non-blazar AGN component which dominates at lower energies, $E_\gamma \lesssim 1$ GeV.

In ABH2, we constrain the blazar population model by simultaneously fitting the DGRB spectrum as well as the blazar flux source count distribution function dN/dF observed by Fermi-LAT [3, 16]. The best fit parameters we find are $q = 4.19_{-0.13}^{+0.57}$, $\log(\kappa/10^{-6}) = 0.38_{-0.70}^{+0.15}$, and $\gamma_1 = 1.51_{-0.09}^{+0.10}$. These are consistent with previous work [8], though more constrained because we are also fitting the source count distribution function dN/dF . The model reproduces the DGRB and blazar dN/dF , with a reduced $\chi^2/\text{DOF} = 0.63$.

Using the dN/dF estimated from a power-law blazar spectrum model is not perfect, since the efficiency depends on this model [16]. However, Ref. [16] tested the dN/dF estimate with a non-power-law fit to the blazar spectra and found it did not appreciably change the estimates of dN/dF , adding a systematic uncertainty of 10%. We also checked this sensitivity with a test fit by increasing the errors on the measured dN/dF at low flux and our model did not prefer a different amplitude or shape to the source counts at the low flux where the efficiency for blazar detection is low.

Our model fits the current DGRB, and, furthermore, predicts the DGRB for the expected enhanced sensitivity to point sources after 5 years of Fermi-LAT data, 2×10^{-9} photons $\text{cm}^{-2} \text{s}^{-1}$, which will resolve $94.7_{-2.1}^{+1.9}\%$ of the flux from blazars. This expected enhanced point source sensitivity value is the Fermi-LAT Collaboration's estimate of the LAT flux sensitivity to point sources at high-latitude with gamma-ray index of ~ 2 [29].¹ In ABH2, we find the 68% and 95% confidence level (CL) upper and lower limit forecasts for the DGRB $E^2 d\Phi/dE$ when varying the fit parameters. This model finds that the DGRB will reduce by a factor of 1.6-2.6 (95% CL) with the spatial point-source resolution of the blazar contribution, after five years of the Fermi-LAT mission. The current and forecast spectra are shown in Fig. 1. In our forecasts, we calculate the limits using the flux as predicted by the model at the minimal and maximal values, not simply performing a scaling of the limits.

From the First to Second Fermi Source Catalogs, there were 162 potentially spurious sources designated, indi-

¹ <http://fermi.gsfc.nasa.gov/science/resources/aosrd/>

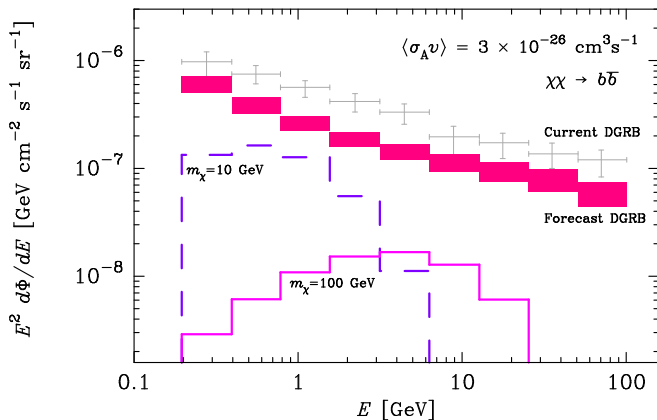


FIG. 1. Shown are the current Fermi-LAT observed DGRB [3] in grey, and the forecast DGRB upper and lower 95% CL central values as the boxed (magenta) regions. Also shown are the expected emission from the Galactic and extragalactic contribution for WIMP annihilation into $b\bar{b}$ for the WIMP particle masses 10 GeV and 100 GeV, for the canonical $\langle\sigma_A v\rangle = 3 \times 10^{-26} \text{ cm}^3 \text{ s}^{-1}$.

cating the sources' further identification with a spatially extended source, source variability, or other systematic effects [30]. The Catalogs include sources with the Test Statistic $TS = 25$, while the Fermi-LAT DGRB analysis only removed sources with $TS = 50$, or with higher significance. (For the definition of TS , see Eq. 20 of Ref. [31].) This type of spurious contamination may alter forecasts for the DGRB, though the higher significance required for the exclusion of sources in the DGRB spectrum would likely reduce or eliminate this systematic effect.

III. CURRENT AND FUTURE SENSITIVITY TO DARK MATTER MODELS OF THE FERMI-LAT DGRB

The signal constrained by observations of the DGRB is the annihilation or decay of dark matter both in the Milky Way Galaxy and extragalactically. There is an irreducible contribution to the background from Galactic annihilation or decay that is isotropic and equal, at minimum, to the emission from the Anti-Galactic-Center (AGC). Here we examine in detail constraints on annihilating and decaying dark matter from both prompt and IC emission of photons.

A. Diffuse Emission from Annihilating Dark Matter

The products of dark matter annihilation emit in gamma rays in several ways: annihilation channels that include the direct emission of a photon, decay of annihilation products into photons, and IC scattering of daughter electrons off of background radiation. Through loop contributions to the annihilation cross-section of dark mat-

ter, it is possible to have a direct $\gamma\gamma$ line signal, through a typically small branching fraction. If the dark matter annihilation particles include hadrons, then the decay chain of the products will lead to neutral pion decay into photons. Additionally, electrons among the dark matter annihilation daughters will up-scatter background photons from the cosmic microwave background (CMB) and starlight to gamma ray energies through IC scattering. We will consider the latter two cases in this paper: photons from prompt radiation in bremsstrahlung and hadronization, and IC emission from electron daughter particles. We calculate the photon and electron spectrum from annihilation using the software PYTHIA [32]. To be conservative, we only consider IC emission from the CMB, not starlight or the infrared (IR) background, which is a good approximation in the direction of the AGC that we will consider.

There are two sources of dark matter that contribute to the DGRB, Galactic and extragalactic dark matter. The signal from Galactic dark matter is largest in the line-of-sight toward the Galactic Center and is much smaller in other directions. However, there is an irreducible, isotropic signal from the Galactic dark matter that is equal to the signal from the AGC. This isotropic signal can be the strongest dark matter contributor to the DGRB given conservative assumptions about the extragalactic contribution [5].

To calculate the dark matter annihilation flux for a given cross-section $\langle\sigma_A v\rangle$ and photon spectrum dN_γ/dE , we follow the treatment of Ref. [6]. The Galactic contribution to the diffuse flux is given by:

$$\frac{d\Phi_\gamma}{dEd\Omega} = \frac{\langle\sigma_A v\rangle}{2} \frac{\mathcal{J}(\text{AGC})}{J_0} \frac{1}{4\pi m_\chi^2} \frac{dN_\gamma}{dE}, \quad (3.1)$$

$$\mathcal{J}(\text{AGC}) = \frac{1}{\Delta\Omega_{\text{obs}}} \int_{\Delta\Omega_{\text{obs}}} \mathcal{J}(0, 180^\circ) d\Omega, \quad (3.2)$$

$$\mathcal{J}(b, \ell) = J_0 \int_{x_{\text{min}}}^{x_{\text{max}}} \rho^2(r_{\text{gal}}(b, \ell, x)) dx, \quad (3.3)$$

$$r_{\text{gal}}(b, \ell, x) = \sqrt{R_\odot^2 - 2xR_\odot \cos(\ell) \cos(b) + x^2}, \quad (3.4)$$

evaluated conservatively at the AGC ($b = 0^\circ$, $\ell = 180^\circ$). In these equations, m_χ is the dark matter particle mass, x is the line-of-sight distance, R_\odot is the distance from the Galactic Center to the sun, and $J_0 \equiv 1/[8.5 \text{ kpc}(0.3 \text{ GeV cm}^{-3})^2]$ is an arbitrary constant that cancels in the final expression for flux. For the Fermi-LAT, the solid angle above $|b| > 10^\circ$ has $\Delta\Omega_{\text{obs}} = 10.4$. The quantity \mathcal{J} is the dark matter density squared integrated along the line-of-sight, and $\mathcal{J}(\text{AGC})$ is this value averaged over the observed angular sky region. For dark matter density ρ we use the minimal Einasto profile for the Milky Way halo:

$$\rho_{\text{Einasto}}(r) = \rho_s \exp \left[-\frac{2}{\alpha_E} \left(\left(\frac{r}{r_s} \right)^{\alpha_E} - 1 \right) \right], \quad (3.5)$$

with $\alpha_E = 0.22$, $r_s = 21 \text{ kpc}$, $r_\odot = 8.28 \text{ kpc}$, and $\rho_\odot = 0.385 \text{ GeV cm}^{-3}$ as in Ref. [6]. This profile is a

conservative choice and gives $\mathcal{J}(\text{AGC}) = 0.62$, and extreme assumptions about the Milky Way dark matter profile only change this value by $\sim 10\%$.

The Milky Way dark matter halo has abundant substructure which enhances the annihilation rate of dark matter. Following Ref. [33], the boost factor for the annihilation due to substructure is

$$B(r) = f_s e^{\Delta^2} + (1 - f_s) \frac{1 + \alpha}{1 - \alpha} \left[\left(\frac{\rho_{\max}}{\rho_h} \right)^{1 - \alpha} - 1 \right]. \quad (3.6)$$

The fraction f_s of the halo volume is filled with a smooth dark matter component with density ρ_h . The maximal density of the PDF ρ_{\max} is taken to be the scale density ρ_s of the earliest forming halos. The first term in Eq. (3.6), $f_s e^{\Delta^2}$, is due to the variation in the smooth component, which contributes only a few percent to the boost, and therefore we ignore it. The second term is the boost factor due to substructure. The total luminosity boost due to the entire Galactic halo within radius R is

$$B(< R) = \frac{\int_0^R B(r) \rho(r)^2 r^2 dr}{\int_0^R \rho(r)^2 r^2 dr}, \quad (3.7)$$

where r is the halo-centric radial coordinate. The annihilation rate is larger in all directions than the AGC, therefore we calculate the luminosity with boost along that line-of-sight as the minimal annihilation rate due to our Galactic halo. Along the line of sight,

$$\mathcal{J}_{\text{boost}}(b, \ell) = \int_{x_{\min}}^{x_{\max}} B(r_{\text{gal}}(b, \ell, x)) \rho^2(r_{\text{gal}}(b, \ell, x)) dx. \quad (3.8)$$

There is a partial reduction of the total luminosity boost [Eq. (3.7)] along the line of sight to the AGC due to our presence within the Galactic halo. Using the central value of $\alpha = 0$ from simulations, the boost is $B_{\text{AGC}} \equiv \mathcal{J}_{\text{boost}}(\text{AGC})/\mathcal{J}(\text{AGC}) = 3.3$. Though the boost factor toward the Galactic Center is expected to be unity [33], that from the total Galactic halo can approach ~ 20 to 2000. Therefore, the approximation of a total Galactic boost in the DGRB field of view as 3.3 is conservative.

In addition to this Galactic contribution to the dark matter flux, we include a sub-dominant contribution from extragalactic dark matter annihilations [34, 35]. This contribution is given by

$$\frac{d\Phi_\gamma}{dE d\Omega} = \frac{\langle \sigma_A v \rangle}{2} \frac{c}{4\pi H_0} \frac{(f_{\text{DM}} \Omega_m)^2 \rho_{\text{crit}}^2}{m_\chi^2} \times \int_0^{z_{\text{up}}} \frac{f(z)(1+z)^3 e^{-\tau(z, E')}}{\sqrt{(1+z)^3 \Omega_m + \Omega_\Lambda}} \frac{dN(E')}{dE'} dz, \quad (3.9)$$

where H_0 is the Hubble constant, Ω_m is the matter density in units of the critical density, ρ_{crit} , and the fraction of matter in dark matter is $f_{\text{DM}} = \Omega_{\text{DM}}/(\Omega_{\text{DM}} + \Omega_b) \approx 0.833$, where we take the fraction of critical density of the dark matter as $\Omega_{\text{DM}} = 0.237$, and baryon density

$\Omega_b = 0.0456$ [36]. Here, $E' = E(1+z)$ is the source energy of the photons, and $z_{\text{up}} = (m_\chi/E) - 1$ is the maximum redshift to get a photon with energy E . The factor $f(z)$ accounts for the increase in density squared during halo growth and the redshift evolution of the halo mass function. We adopt the fit of Refs. [35, 37], namely:

$$f(z) = f_0 10^{0.9[\exp(-0.9z) - 1] - 0.16z}. \quad (3.10)$$

For the Einasto profile, $f_0 \simeq 3 \times 10^4$. We also include the boost factor of 6.6, from the total luminosity of a halo $B(< R)$. This extragalactic contribution only accounts for $\lesssim 30\%$ of the total diffuse flux from dark matter.

To calculate the limits on $\langle \sigma v \rangle$, we attribute all the DGRB to dark matter annihilation (or decay), including both the Galactic and extragalactic dark matter contributions. This provides an upper limit on the cross-section of annihilating dark matter (or a lower limit on the lifetime of decaying dark matter). We use the upper and lower 68% and 95% CL forecast fluxes corresponding to the extremal upper and lower fluxes in the three-dimensional contour in q , κ and γ_1 parameter space, as constrained by the DGRB spectrum and source count distribution function, as described in our companion paper [14]. We take errors on the forecast DGRB for all of the upper and lower 68% and 95% CL forecast fluxes each to be proportional to its amplitude, which corresponds to the modeling methods of the DGRB measurement, though this is not necessarily the ultimate scaling of the errors. To do so, a Monte Carlo of the modeling methods of Ref. [3] would need to be performed, which is beyond the scope of this work.

Fig. 2 demonstrates the forecast for four canonical dark matter annihilation channels and how they compare to expected minimal supersymmetric model (MSSM) and minimal supergravity (mSUGRA) dark matter cross sections. The cross sections are from a scan in MSSM and mSUGRA parameter space by Ref. [38]. Note that our predicted constraints from Fermi-LAT's observations of the DGRB are comparable to current constraints Fermi-LAT observations of the Galactic Center [23], shown as a dashed line in Fig. 2. For comparison, in Fig. 2 we also show constraints from the Fermi-LAT analysis of stacked dwarf galaxies [39, 40]. The constraints shown are from Ref. [40]. In all relevant panels, we also show constraints from the HESS observation of the Galactic Center [41] as calculated in Ref. [42].

It has been proposed that a nonthermally-produced wino-like dark matter annihilation could lead to the positron excess signal in PAMELA, which requires wino dark matter masses of $100 \text{ GeV} \lesssim m_\chi \lesssim 200 \text{ GeV}$ [22]. As shown in Fig. 2(b), these models are disfavored by the current constraints, and the forecast spectrum will be significantly more sensitive to this model.

The standard thermal relic weakly-interacting dark matter annihilation cross section is $\sim 3 \times 10^{-26} \text{ cm}^3 \text{ s}^{-1}$ [45], which corresponds roughly with the broader MSSM/mSUGRA region. The plot of dark matter annihilating into $\tau^+ \tau^-$, Fig. 2(d), contains a region in param-

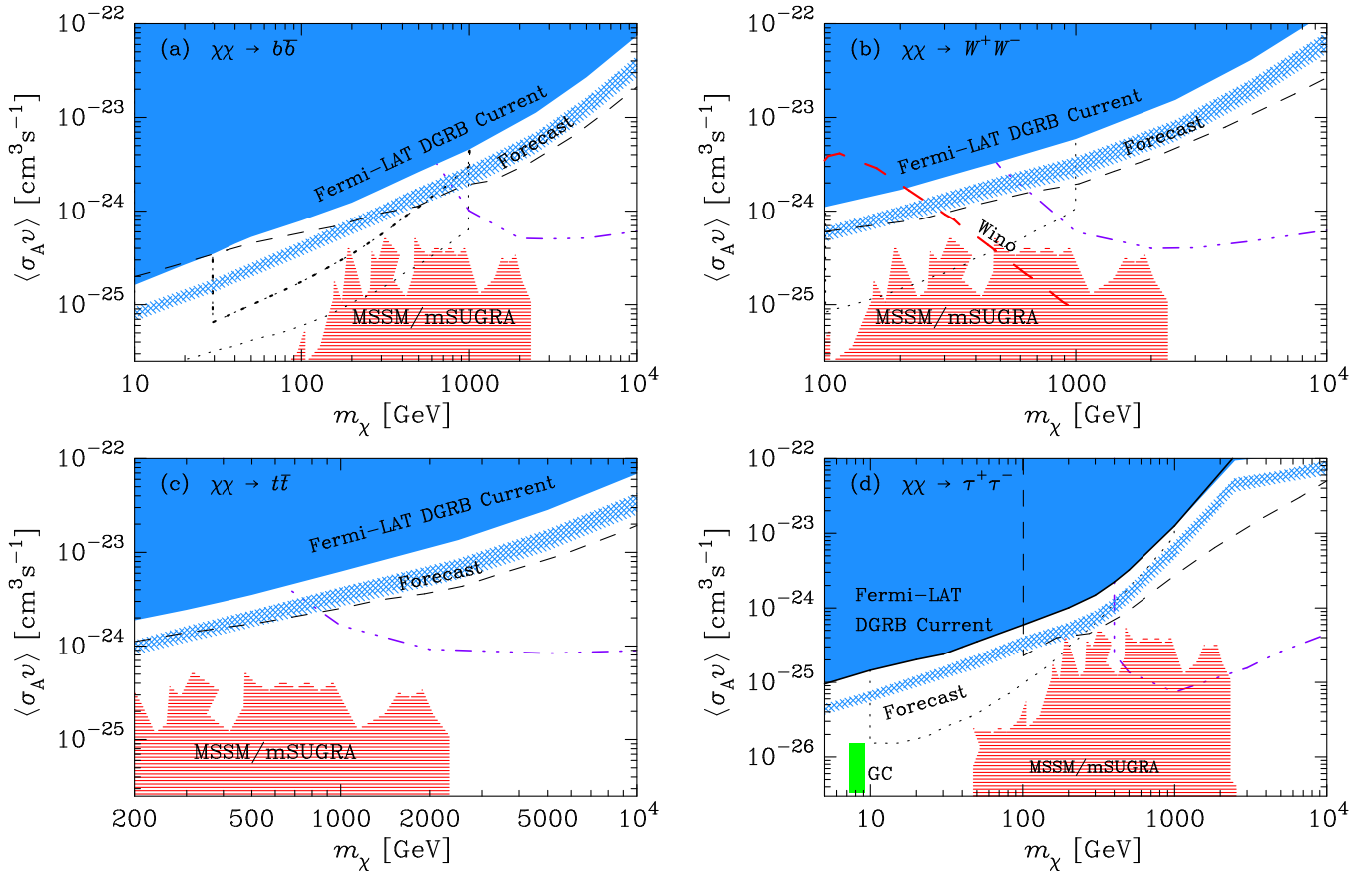


FIG. 2. Shown are our predictions for the Fermi-LAT sensitivity to constraints on dark matter in several canonical annihilation channels: (a) $\chi\chi \rightarrow b\bar{b}$; (b) $\chi\chi \rightarrow W^+W^-$; (c) $\chi\chi \rightarrow t\bar{t}$; (d) $\chi\chi \rightarrow \tau^+\tau^-$. The blue double and single hashed regions are the 68% and 95% CL predictions for 5-year Fermi-LAT sensitivity, respectively. Also shown is the limit from the current Fermi-LAT DGRB spectrum (solid blue). In panel (a), we also show the current constraints from Fermi-LAT observations of Draco (thick dotted line) [43]. In panels (a), (b) and (d), we show constraints from the stacking of dwarf galaxies (thin dotted line) [40]. In the W^+W^- channel, panel (b), the cross-section versus mass for a non-thermal wino-like neutralino is shown. The wino-like dark matter of the PAMELA signal at $m_\chi \sim 200$ GeV [22] is disfavored by the current constraints and will be further constrained in the forecast spectrum. The ‘MSSM/mSUGRA’ red-striped region is the expected cross-sections for a sampling of points in supersymmetric parameter space [38]. The dashed line is a limit from the $3^\circ \times 3^\circ$ in the Galactic Center [23]. In the $\tau^+\tau^-$ plot, panel (d), the green box is a region that could be consistent with an excess in the spectrum toward the Galactic Center [44]. In all panels, the triple-dot-dashed line is the limit from the HESS observation of the Galactic Center [41] for the respective channels in the case of a Navarro-Frenk-White halo profile, from Ref. [42].

eter space which has recently been claimed to be consistent with the morphology and spectrum of excess gamma ray flux towards the Galactic Center [44], though such a signal is also consistent with emission from stellar clusters [46]. The width of the forecast region follows from the increasing width of the DGRB prediction with energy. Our model predicts a factor of 2 – 3 (95% CL) improvement in the sensitivity of the DGRB measurement to dark matter.

B. Diffuse Emission from Annihilation of Dark Matter into Leptonic Modes and IC

Dark matter that annihilates into leptons has been proposed as an explanation for an excess in cosmic-ray

positrons seen by the PAMELA collaboration [49] and a feature in the cosmic-ray e^+/e^- spectrum from the Fermi-LAT [50]. The DGRB is forecast to be sensitive to direct $\mu^+\mu^-$ production models that fit the PAMELA excess and Fermi-LAT e^+/e^- feature, such as Asymmetric Dark Matter [21]. Such direct annihilation models are already strongly disfavored by constraints of observations by the Galactic Ridge by HESS [6, 51, 52], observations by Fermi-LAT toward the Galactic Center [23], and HESS toward the Galactic Center [41, 42]. The latter two constraints shown in Fig. 3.

It has also been suggested that Sommerfeld-enhanced dark matter annihilation into four leptons, via a light mediator particle, could explain these signals. Therefore, we also consider how an improved DGRB will affect these leptonic dark matter annihilation channels. Note

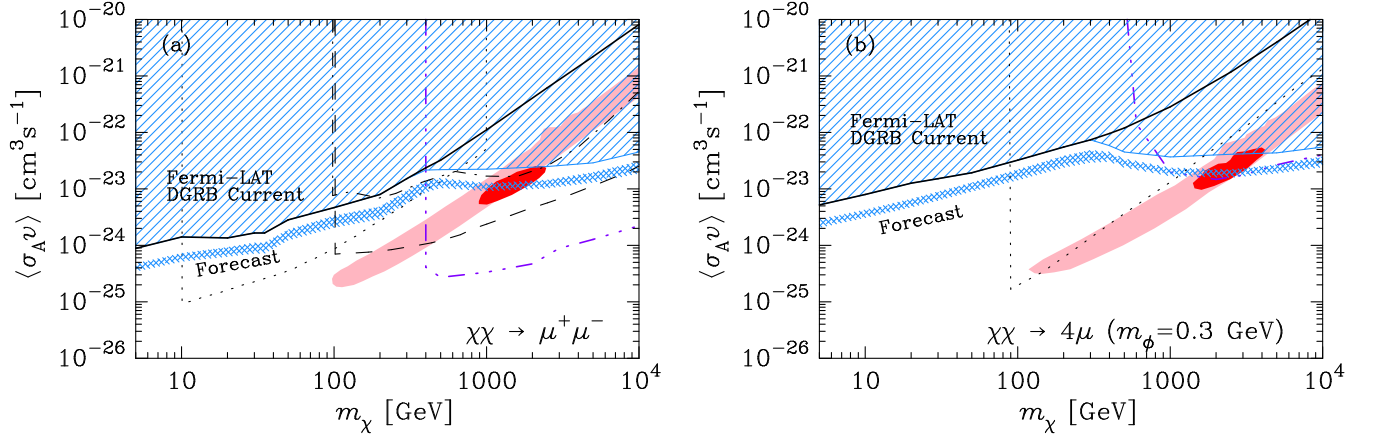


FIG. 3. Shown in panel (a) are our predictions for Fermi-LAT sensitivity to $\mu^+\mu^-$ channel dark matter annihilation. The dot-dashed line is the 95% CL limit on prompt and IC emission from Ursa Minor [43]. In this panel, we show the constraint from the stacking of dwarf galaxies (thin dotted line) [40]. In panel (b), dark matter annihilation into four muons via intermediate 0.3 GeV scalar particles ϕ . The blue double and single hashed regions are the 68% and 95% CL predictions for 5-year Fermi-LAT sensitivity, respectively. Also included is the limit from the current Fermi-LAT DGRB spectrum (striped blue region). The solid black line shows where the exclusion would be without the IC contribution. The light pink shaded region is consistent with a dark matter interpretation of the PAMELA signal and the dark red shaded region is consistent with a dark matter interpretation of the Fermi-LAT e^+/e^- feature [47, 48]. The triple-dot-dashed line is the limit from the HESS observation of the Galactic Center [41] for the respective channels in the case of a Navarro-Frenk-White halo profile, from Ref. [42]. In panel (b), the dotted line is a limit on dark matter annihilation from radio synchrotron from the Galactic Center [47]. The dashed line is the 99% CL limit from the $3^\circ \times 3^\circ$ region toward the Galactic Center [23].

that such models are also constrained by detailed calculations of the relic abundance from dark matter production in the early universe and halo shapes [53], as well as distortions of the CMB spectrum [54]. Recent work finds that several reasonable parameter choices in models of Sommerfeld-enhanced dark matter for PAMELA and the Fermi-LAT e^+/e^- spectral feature avoid these limits [55]. These Sommerfeld-enhanced models are partially constrained by the current limits and will be further constrained by our forecast limits, as shown in Fig. 3(b).

Dark matter annihilation into leptons produces fewer photons than the quark or gauge boson channels. However, such annihilations do produce highly-boosted electrons which undergo IC scattering on the CMB and starlight which is then observable in gamma rays. We calculate this IC contribution as in Ref. [23]. To be conservative, we only include the scattering from the CMB, not from starlight or the IR background.

The spectrum of IC photons coming from one dark matter annihilation is given by [23, 27]

$$\frac{dN}{dE} = \frac{1}{E} \int_{m_e}^{m_\chi} d\epsilon \frac{\mathcal{P}(E, \epsilon)}{\dot{\mathcal{E}}(\epsilon)} Y(\epsilon), \quad (3.11)$$

where $\mathcal{P}(E, \epsilon)$ is the differential power emitted into photons of energy E by an electron with energy ϵ , $\dot{\mathcal{E}}$ denotes the total rate of electron energy loss due to IC scattering, and $Y(\epsilon)$ is the number of electrons generated with energy larger than ϵ in one annihilation. To get the energy of the annihilation products, we use the software PYTHIA [32]. In the Thomson limit, which is a very

good approximation for CMB photons, one obtains

$$\dot{\mathcal{E}}(\epsilon) = \frac{4}{3} \sigma_T \gamma^2 \int_0^\infty d\epsilon' \epsilon' n(\epsilon') \quad (3.12)$$

$$\mathcal{P}(E, \epsilon) = \frac{3\sigma_T}{4\gamma^2} E \int_0^1 dy \frac{n(\epsilon'(y))}{y} \times (2y \ln y + y + 1 - 2y^2), \quad (3.13)$$

where γ is the Lorentz factor of the electron, ϵ' is the energy of the initial CMB photon, $y \equiv E/(4\gamma^2\epsilon')$, $\sigma_T \simeq 0.665$ barn is the Thomson cross section, and the radiation density of CMB photons at $T_{\text{CMB}} \simeq 2.725$ K is given by

$$n_{\text{CMB}}(\epsilon') = \frac{\epsilon'^2}{\pi^2} \frac{1}{\exp(\epsilon'/T_{\text{CMB}}) - 1}. \quad (3.14)$$

The flux coming from the IC contribution can then be calculated as in Eqs. (3.1)-(3.10).

It is important to note that we are neglecting the diffusion of the electrons and positrons from the dark matter annihilation to the point where IC scattering occurs. As stated in Ref. [23], this is a good approximation in regions away from the Galactic Center, as we consider in this work. For an analysis where diffusion is included, see Ref. [48]. To be more explicit, in Ref. [56], it was shown that the electron/positron flux produced by dark matter annihilations was only slightly modified by diffusion effects for distances from the Galactic Center larger than 8 kpc. Corrections were found to reach a factor of 2 only at the lowest energies around 100 MeV (see their

Fig. 14). Therefore, diffusion effects are not significant in our calculation of the IC component. Note that the IC component is modeled in the measurement if the DGRB is independent of the observation [3], so there is no accidental subtraction of a potential IC signal.

Our calculations for the standard $\mu^+\mu^-$ leptonic channel are shown in Fig. 3(a). Also shown are the regions which are consistent with the PAMELA excess and Fermi-LAT e^+/e^- spectral feature from Ref. [47], modified for a higher local dark matter density of our minimal Einasto halo model ($\rho_\odot = 0.385 \text{ GeV cm}^{-3}$), and the local boost of $B(r = R_\odot) = 1.57$ [Eq. (3.6)] from substructure. For this boost, we use the same parameters for the subhalo PDF as our subhalo boost annihilation signal. Such models are already highly constrained by several gamma ray observations as shown in Fig. 3(a), and such models will be further constrained with our forecast DGRB sensitivity. Note that the IC contribution improves the bounds by several orders of magnitude. The IC gamma ray flux contribution peaks at much lower energies than the prompt component for a given dark matter particle mass, which is why the width of the forecast region decreases when the IC component becomes important. Also shown in Fig. 3 are complementary limits on the cross-section of $\mu^+\mu^-$ -channel annihilating dark matter from other work. Shown in Fig. 3(b) is dark matter annihilation into four muons via intermediate scalars ϕ with 0.3 GeV masses. Even in this less-constrained case, our forecast is that the Fermi-LAT measurement of the DGRB will have the sensitivity to detect or rule out a portion of the parameter space the dark matter interpretations of PAMELA.

C. Diffuse Emission from Decaying Dark Matter

Decaying dark matter is another, less constrained, possibility for the source of the positron fraction signal seen in PAMELA and the Fermi-LAT e^+/e^- spectral feature [23]. To calculate the flux from decaying dark matter with lifetime τ and photon spectrum dN_γ/dE , the procedure is very similar to the annihilating dark matter case. However, in Eq. (3.3), $\rho^2 \rightarrow \rho$ and there is no boost factor due to the lack of decay enhancement with density. Here, Eq. (3.1) becomes

$$\frac{d\Phi_\gamma}{dEd\Omega} = \frac{1}{\tau} \frac{J_{\text{AGC}}}{J_0} \frac{1}{4\pi m_\chi} \frac{dN_\gamma}{dE}. \quad (3.15)$$

Similarly, to calculate the extragalactic flux from decaying dark matter, in Eq. (3.9) replace

$$\frac{\langle \sigma_A v \rangle}{2} \frac{(f_{\text{DM}} \Omega_m)^2 \rho_{\text{crit}}^2}{m_\chi^2} \rightarrow \frac{1}{\tau} \frac{(f_{\text{DM}} \Omega_m) \rho_{\text{crit}}}{m_\chi} \quad (3.16)$$

and drop all boost factors.

Fig. 4 shows how the predicted DGRB value will constrain the lifetime of a dark matter particle which decays into $\mu^+\mu^-$. The improved constraint will have the

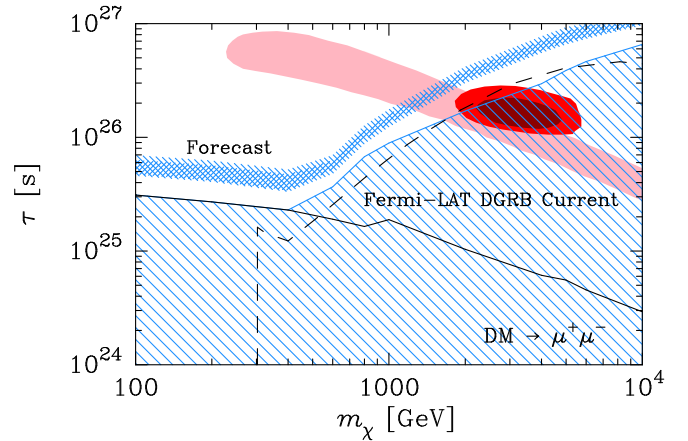


FIG. 4. Our predictions for Fermi-LAT sensitivity to dark matter decaying into $\mu^+\mu^-$. The dark and light blue hashed regions are the 68% and 95% CL predictions for 5-year Fermi-LAT sensitivity, respectively. Also included is the limit from the current Fermi-LAT DGRB spectrum (blue striped region). The solid black line shows where the exclusion would be without the IC contribution. The light pink shaded region is consistent with a dark matter interpretation of the PAMELA signal, and the dark red shaded regions are consistent with a dark matter interpretation of the Fermi-LAT e^+/e^- feature at 3- and 5- σ [48]. The dashed line is from constraints on prompt and IC emission from dark matter annihilation made from Fermi-LAT observations of the Fornax cluster of galaxies [57].

sensitivity to exclude or detect the decaying dark matter interpretation of the Fermi-LAT e^+/e^- feature and should provide strong limits on an interpretation of the PAMELA excess [48, 49]. The DGRB limit is comparable to and is forecast to be more sensitive than the limits on decaying dark matter from Fermi-LAT observations of clusters of galaxies [57], as shown in Fig. 4.

D. Comparison to Direct Dark Matter Detection Limits on Light Dark Matter

Dark matter may be detected through two distinct methods: indirect detection experiments seek the annihilation or decay products from dark matter in the universe, while direct detection experiments look for the recoil of heavy nuclei after their collision with a dark matter particle from our Galactic halo. In general, the interaction cross-section between annihilating dark matter is not simply related to the interaction cross-section between dark matter and nucleons. A few recent direct-detection experiments, however, have seen signals that could be caused by a light dark matter particle, including DAMA [60–62, 64], CoGeNT [59] and CDMS [63].

These light dark matter signals could be due to dark matter that interacts through the exchange of Higgs bosons [24, 25]. For such a dark matter candidate, the in-

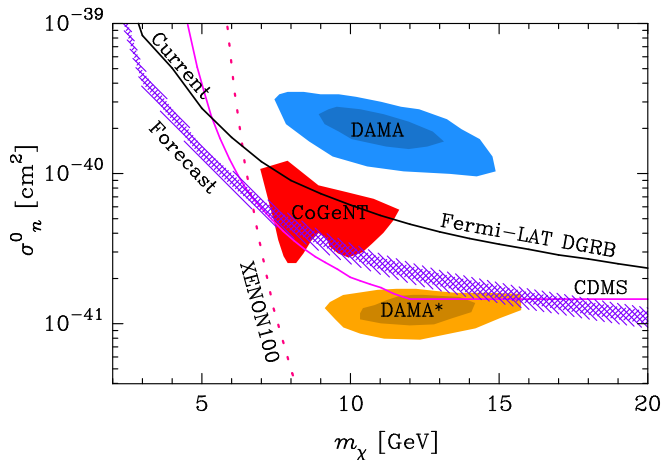


FIG. 5. Our predictions for Fermi-LAT sensitivity to light dark matter coupled via Higgs-like couplings [25]. The dark and light purple hashed regions are the 68% and 95% CL predictions for 5-year Fermi-LAT sensitivity, respectively. Also included is the limit from the current Fermi-LAT DGRB spectrum (black line). To the right of the dotted pink line is exclusion from the XENON100 collaboration [58]. The red ‘CoGeNT’ region is consistent with the findings of the CoGeNT collaboration [59]. The blue upper ‘DAMA’ region is the DAMA signal without channeling [60]. The orange lower ‘DAMA*’ region is the DAMA signal if channeling is included [61, 62]. The region labeled ‘CDMS’ is excluded by that experiment’s light dark matter search at 95% CL [63].

direct annihilation cross section and direct nuclear cross-section are related by

$$\sigma_{\text{ind}}(SS \rightarrow \bar{f}f) \frac{v}{c} = n_c \frac{\lambda_L^2}{\pi} \frac{m_f^2 (m_S^2 - m_f^2)^{3/2}}{m_h^4 m_S^3} \quad (3.17)$$

$$\sigma_{\text{dir}}(SN \rightarrow SN) = \frac{\lambda_L^2}{\pi} \frac{\mu_r^2}{m_h^4 m_S^2} f^2 m_N^2 \quad (3.18)$$

$$\sum \frac{\sigma_{\text{ind}}}{\sigma_{\text{dir}}} \frac{v}{c} = \sum \frac{n_c m_f^2}{f^2 m_N^2} \frac{(m_S^2 - m_f^2)^{3/2}}{\mu_r^2 m_S} \quad (3.19)$$

where m_h is the Higgs mass, λ_L is the dark matter-Higgs coupling, $n_c = 3(1)$ for quarks (leptons), μ_r is the dark matter-nucleon reduced mass, $f \sim 0.3$, and m_S is the dark matter mass [25]. The sum in Eq. (3.19) is over all annihilation products, which are dominated by the b -quark, the c -quark, and the τ -lepton. Through this ratio, we can relate our predicted DGRB limits on indirect detection into limits on direct detection experiments. For such a Higgs-mediated dark matter model, we compare our projected limit to the findings of several direct detection experiments in Fig. 5.

The limit on the dark matter-nucleon cross-section as found by our DGRB forecast is competitive with the limits by the XENON100 collaboration in the lowest mass range [58]. The current Fermi-LAT DGRB values rule

out the DAMA region without channeling and some of the region consistent with a dark matter interpretation of CoGeNT. After a Fermi-LAT 5-year run, we forecast the DGRB spectrum to have the sensitivity to exclude most of the CoGeNT region consistent with dark matter interpretations in the spin-independent case. This is complementary to the findings of direct detection experiments since the DGRB indirect-detection limits tend to exclude lower dark matter masses than direct-detection experiments.

IV. CONCLUSIONS

The DGRB as measured by Fermi-LAT is one of the most powerful constraints on annihilating weak-scale particle dark matter. We show that the likely resolution of blazars into point sources by Fermi-LAT—and their automatic removal from the DGRB measurement—will enhance the sensitivity of the DGRB to dark matter annihilation by a factor of 2 to 3 (95% CL), depending on the channel, mass scale, and true realization of the blazar distribution and SED sequence.

We find the forecast dark matter sensitivity of the DGRB observation to both prompt and inverse-Compton photon emission to be comparable in sensitivity with other limits on annihilating weak-scale dark matter. The DGRB is forecast to be comparable to current limits from Fermi-LAT observations toward the Galactic Center [23], individual dwarf galaxies [43], and, in the case of decaying dark matter, observations of clusters of galaxies [57]. This sensitivity makes the DGRB among the best methods of detecting or constraining dark matter with the Fermi-LAT mission. The forecast for the DGRB projects it to be less constraining, for certain channels and particle masses, than current stacked dwarf analyses with Fermi-LAT [39, 40] and observations of the Galactic Center by HESS [41, 42].

The future resolution and reduction of the DGRB into blazar point sources highlights and enhances the possibility that the Fermi-LAT experiment will either detect or constrain the dark matter in a robust yet conservative way.

ACKNOWLEDGMENTS

We would like to thank P. Agrawal, J. Beacom, Z. Chacko, J. McEnery and N. Weiner for useful discussions. KNA and JPH are supported by NSF Grant 07-57966 and NSF CAREER Award 09-55415. This work has been partially supported by MICNN, Spain, under contracts FPA 2007-60252 and Consolider-Ingenio CPAN CSD2007-00042 and by the the Comunidad de Madrid through Proyecto HEPHACOS ESP-1473. S.B. acknowledges support from the CSIC grant JAE-DOC.

-
- [1] J. L. Feng, *Ann.Rev.Astron.Astrophys.* **48**, 495 (2010), arXiv:1003.0904 [astro-ph.CO].
- [2] E. A. Baltz *et al.*, *JCAP* **0807**, 013 (2008), arXiv:0806.2911 [astro-ph].
- [3] A. A. Abdo *et al.* (Fermi-LAT Collaboration), *Phys. Rev. Lett.* **104**, 101101 (2010), arXiv:1002.3603 [astro-ph.HE].
- [4] A. A. Abdo *et al.* (Fermi-LAT), *JCAP* **1004**, 014 (2010), arXiv:1002.4415 [astro-ph.CO].
- [5] G. D. Mack, T. D. Jacques, J. F. Beacom, N. F. Bell, and H. Yuksel, *Phys. Rev.* **D78**, 063542 (2008), arXiv:0803.0157 [astro-ph].
- [6] K. N. Abazajian, P. Agrawal, Z. Chacko, and C. Kilic, *JCAP* **1011**, 041 (2010), arXiv:1002.3820 [astro-ph.HE].
- [7] F. Stecker and M. Salamon, *Astrophys.J.* **464**, 600 (1996), arXiv:astro-ph/9601120 [astro-ph].
- [8] Y. Inoue and T. Totani, *Astrophys. J.* **702**, 523 (2009), arXiv:0810.3580 [astro-ph].
- [9] J. Singal, V. Petrosian, and M. Ajello, (2011), arXiv:1106.3111 [astro-ph.CO].
- [10] M. Cavadini, R. Salvaterra, and F. Haardt, (2011), arXiv:1105.4613 [astro-ph.CO].
- [11] B. D. Fields, V. Pavlidou, and T. Prodanovic, *Astrophys.J.* **722**, L199 (2010), arXiv:1003.3647 [astro-ph.CO].
- [12] C. A. Faucher-Giguere and A. Loeb, *JCAP* **1001**, 005 (2010), arXiv:0904.3102 [astro-ph.HE].
- [13] Y. Inoue *et al.*, (2010), arXiv:1001.0103 [astro-ph.HE].
- [14] K. N. Abazajian, S. Blanchet, and J. Harding, *Phys.Rev.* **D84**, 103007 (2011), (ABH2), arXiv:1012.1247 [astro-ph.CO].
- [15] G. Fossati, A. Celotti, G. Ghisellini, and L. Maraschi, *Mon. Not. Roy. Astron. Soc.* **289**, 136 (1997), arXiv:astro-ph/9704113 [astro-ph]; G. Fossati, L. Maraschi, A. Celotti, A. Comastri, and G. Ghisellini, *ibid.* **299**, 433 (1998), arXiv:astro-ph/9804103 [astro-ph]; D. Donato, G. Ghisellini, G. Tagliaferri, and G. Fossati, *Astron. & Astrophys.* **375**, 739 (2001), arXiv:astro-ph/0105203 [astro-ph].
- [16] A. A. Abdo *et al.* (Fermi-LAT Collaboration), *Astrophys.J.* **720**, 435 (2010), arXiv:1003.0895 [astro-ph.CO].
- [17] T. M. Venters and V. Pavlidou, *Astrophys.J.* **737**, 80 (2011), arXiv:1105.0372 [astro-ph.HE].
- [18] F. W. Stecker and T. M. Venters, *Astrophys.J.* **736**, 40 (2011), arXiv:1012.3678 [astro-ph.HE].
- [19] A. Neronov and D. Semikoz, (2011), arXiv:1103.3484 [astro-ph.CO].
- [20] N. Arkani-Hamed, D. P. Finkbeiner, T. R. Slatyer, and N. Weiner, *Phys. Rev.* **D79**, 015014 (2009), arXiv:0810.0713 [hep-ph]; M. Pospelov and A. Ritz, *Phys.Lett.* **B671**, 391 (2009), arXiv:0810.1502 [hep-ph].
- [21] A. Falkowski, J. T. Ruderman, and T. Volansky, *JHEP* **1105**, 106 (2011), arXiv:1101.4936 [hep-ph]; Y. Cai, M. A. Luty, and D. E. Kaplan, (2009), arXiv:0909.5499 [hep-ph].
- [22] P. Grajek, G. Kane, D. J. Phalen, A. Pierce, and S. Watson, (2008), arXiv:0807.1508 [hep-ph]; G. Kane, R. Lu, and S. Watson, *Phys.Lett.* **B681**, 151 (2009), arXiv:0906.4765 [astro-ph.HE].
- [23] M. Cirelli, P. Panci, and P. D. Serpico, *Nucl.Phys.* **B840**, 284 (2010), arXiv:0912.0663 [astro-ph.CO].
- [24] C. Burgess, M. Pospelov, and T. ter Veldhuis, *Nucl.Phys.* **B619**, 709 (2001), arXiv:hep-ph/0011335 [hep-ph].
- [25] S. Andreas, T. Hambye, and M. H. Tytgat, *JCAP* **0810**, 034 (2008), arXiv:0808.0255 [hep-ph]; C. Arina and M. H. Tytgat, *ibid.* **1101**, 011 (2011), arXiv:1007.2765 [astro-ph.CO].
- [26] K. N. Abazajian, M. Markevitch, S. M. Koushiappas, and R. C. Hickox, *Phys. Rev.* **D75**, 063511 (2007), arXiv:astro-ph/0611144.
- [27] S. Profumo and T. E. Jeltema, *JCAP* **0907**, 020 (2009), arXiv:0906.0001 [astro-ph.CO].
- [28] Y. Ueda, M. Akiyama, K. Ohta, and T. Miyaji, *Astrophys. J.* **598**, 886 (2003), arXiv:astro-ph/0308140.
- [29] W. Atwood *et al.* (LAT Collaboration), *Astrophys.J.* **697**, 1071 (2009), arXiv:0902.1089 [astro-ph.IM].
- [30] A. Abdo *et al.* (Fermi-LAT Collaboration), (2011), arXiv:1108.1435 [astro-ph.HE].
- [31] J. Mattox, D. Bertsch, J. Chiang, B. Dingus, S. Digel, *et al.*, *Astrophys.J.* **461**, 396 (1996).
- [32] T. Sjostrand, S. Mrenna, and P. Z. Skands, *JHEP* **05**, 026 (2006), arXiv:hep-ph/0603175.
- [33] M. Kamionkowski, S. M. Koushiappas, and M. Kuhlen, *Phys. Rev.* **D81**, 043532 (2010), arXiv:1001.3144 [astro-ph.GA].
- [34] L. Bergstrom, J. Edsjo, and P. Ullio, *Phys. Rev. Lett.* **87**, 251301 (2001), arXiv:astro-ph/0105048.
- [35] P. Ullio, L. Bergstrom, J. Edsjo, and C. G. Lacey, *Phys. Rev.* **D66**, 123502 (2002), arXiv:astro-ph/0207125.
- [36] E. Komatsu *et al.* (WMAP Collaboration), *Astrophys.J.Suppl.* **192**, 18 (2011), arXiv:1001.4538 [astro-ph.CO].
- [37] S. Ando, *Phys. Rev. Lett.* **94**, 171303 (2005), arXiv:astro-ph/0503006; H. Yuksel, S. Horiuchi, J. F. Beacom, and S. Ando, *Phys. Rev.* **D76**, 123506 (2007), arXiv:0707.0196 [astro-ph].
- [38] L. Bergstrom, T. Bringmann, and J. Edsjo, *Phys.Rev.* **D83**, 045024 (2011), arXiv:1011.4514 [hep-ph].
- [39] A. Geringer-Sameth and S. M. Koushiappas, *Phys.Rev.Lett.* **107**, 241303 (2011), arXiv:1108.2914 [astro-ph.CO].
- [40] M. Ackermann *et al.* (Fermi-LAT collaboration), *Phys.Rev.Lett.* **107**, 241302 (2011), arXiv:1108.3546 [astro-ph.HE].
- [41] A. Abramowski *et al.* (The HESS), *Phys.Rev.Lett.* **106**, 161301 (2011), arXiv:1103.3266 [astro-ph.HE].
- [42] K. N. Abazajian and J. Harding, (2011), arXiv:1110.6151 [hep-ph].
- [43] A. Abdo, M. Ackermann, M. Ajello, W. Atwood, L. Baldini, *et al.*, *Astrophys.J.* **712**, 147 (2010), arXiv:1001.4531 [astro-ph.CO].
- [44] D. Hooper and L. Goodenough, *Phys.Lett.* **B697**, 412 (2011), arXiv:1010.2752 [hep-ph].
- [45] Y. B. Zeldovich, *Zh. Eksp. Teor. Fiz.* **48**, 986 (1965); G. Steigman, *Ann. Rev. Nucl. Part. Sci.* **29**, 313 (1979); R. J. Scherrer and M. S. Turner, *Phys. Rev. D* **33**, 1585 (1986).
- [46] K. N. Abazajian, *JCAP* **1103**, 010 (2011), arXiv:1011.4275 [astro-ph.HE].
- [47] P. Meade, M. Papucci, and T. Volansky, *JHEP* **12**, 052 (2009), arXiv:0901.2925 [hep-ph].
- [48] M. Papucci and A. Strumia, *JCAP* **1003**, 014 (2010), arXiv:0912.0742 [hep-ph].
- [49] O. Adriani *et al.* (PAMELA Collaboration), *Nature* **458**,

- 607 (2009), arXiv:0810.4995 [astro-ph].
- [50] A. A. Abdo *et al.* (Fermi-LAT Collaboration), Phys. Rev. Lett. **102**, 181101 (2009), arXiv:0905.0025 [astro-ph.HE]; D. Grasso *et al.* (FERMI-LAT Collaboration), Astropart.Phys. **32**, 140 (2009), arXiv:0905.0636 [astro-ph.HE]; T. R. Slatyer, N. Padmanabhan, and D. P. Finkbeiner, Phys.Rev. **D80**, 043526 (2009), arXiv:0906.1197 [astro-ph.CO].
 - [51] F. Aharonian *et al.* (HESS), Nature **439**, 695 (2006), arXiv:astro-ph/0603021.
 - [52] G. Bertone, M. Cirelli, A. Strumia, and M. Taoso, JCAP **0903**, 009 (2009), arXiv:0811.3744 [astro-ph].
 - [53] J. L. Feng, M. Kaplinghat, and H.-B. Yu, Phys.Rev.Lett. **104**, 151301 (2010), arXiv:0911.0422 [hep-ph].
 - [54] S. Galli, F. Iocco, G. Bertone, and A. Melchiorri, Phys.Rev. **D80**, 023505 (2009), arXiv:0905.0003 [astro-ph.CO]; J. Zavala, M. Vogelsberger, and S. D. White, *ibid.* **D81**, 083502 (2010), arXiv:0910.5221 [astro-ph.CO].
 - [55] D. P. Finkbeiner, L. Goodenough, T. R. Slatyer, M. Vogelsberger, and N. Weiner, JCAP **1105**, 002 (2011), arXiv:1011.3082 [hep-ph].
 - [56] L. Pieri, J. Lavalle, G. Bertone, and E. Branchini, Phys.Rev. **D83**, 023518 (2011), arXiv:0908.0195 [astro-ph.HE].
 - [57] L. Dugger, T. E. Jeltema, and S. Profumo, JCAP **1012**, 015 (2010), arXiv:1009.5988 [astro-ph.HE].
 - [58] E. Aprile *et al.* (XENON100 Collaboration), Phys.Rev. **D84**, 052003 (2011), arXiv:1103.0303 [hep-ex].
 - [59] C. Aalseth *et al.* (CoGeNT collaboration), Phys.Rev.Lett. **106**, 131301 (2011), arXiv:1002.4703 [astro-ph.CO].
 - [60] C. Savage, G. Gelmini, P. Gondolo, and K. Freese, Phys.Rev. **D83**, 055002 (2011), arXiv:1006.0972 [astro-ph.CO].
 - [61] J. Kopp, T. Schwetz, and J. Zupan, JCAP **1002**, 014 (2010), arXiv:0912.4264 [hep-ph].
 - [62] B. Feldstein, A. Fitzpatrick, E. Katz, and B. Tweedie, JCAP **1003**, 029 (2010), arXiv:0910.0007 [hep-ph].
 - [63] Z. Ahmed *et al.* (CDMS-II Collaboration), Phys.Rev.Lett. **106**, 131302 (2011), arXiv:1011.2482 [astro-ph.CO].
 - [64] R. Bernabei *et al.* (DAMA Collaboration), Eur.Phys.J. **C56**, 333 (2008), arXiv:0804.2741 [astro-ph].